

# Noninvasive identification of epicardial ventricular tachycardia substrate by magnetic resonance–based signal intensity mapping



Ángel Arenal, MD, PhD,<sup>\*</sup> Esther Pérez-David, MD,<sup>\*</sup> Pablo Ávila, MD,<sup>\*</sup> Javier Fernández-Portales, MD,<sup>†</sup> Verónica Crisóstomo, DVM, PhD,<sup>†</sup> Claudia Báez, DVM,<sup>†</sup> Javier Jiménez-Candil, MD, PhD,<sup>†</sup> José L. Rubio-Guivernau, PhD,<sup>‡</sup> María J. Ledesma-Carbayo, PhD,<sup>‡</sup> Gerard Loughlin, MD,<sup>\*</sup> Javier Bermejo, MD, PhD,<sup>\*</sup> Francisco M. Sánchez-Margallo, DVM, PhD,<sup>†</sup> Francisco Fernández-Avilés, MD, PhD<sup>\*</sup>

From the <sup>\*</sup>Hospital General Universitario Gregorio Marañón, Madrid, Spain, <sup>†</sup>Centro de Cirugía de Mínima Invasión Jesús Usón, Cáceres, Spain, and <sup>‡</sup>Universidad Politécnica de Madrid and CIBER-BBN, Spain.

**BACKGROUND** Endo-epicardial substrate ablation reduces ventricular tachycardia (VT) recurrences; however, not all patients in whom the epicardium is explored have a VT substrate. Contrast-enhanced magnetic resonance imaging (ceMRI) is used to characterize VT substrate after myocardial infarction.

**OBJECTIVE** The purpose of this study was to determine if epicardial VT substrate can be identified noninvasively by ceMRI-based endo-epicardial signal intensity (SI) mapping.

**METHODS** Myocardial infarction was induced in 31 pigs. Four or 16 weeks later, ceMRI was obtained, and the averaged subendocardial and subepicardial SIs were projected onto 3-dimensional endocardial and epicardial shells in which dense scar, heterogeneous tissue (HT), and normal tissue were differentiated. An HT channel was defined as a corridor of HT surrounded by dense scar and connected to normal tissue. A “patchy” scar pattern was defined as the presence of at least 3 dense scar islets surrounded by HT forming  $\geq 2$  HT channels. Electrophysiologic study was performed after ceMRI.

**RESULTS** Thirty-three different sustained monomorphic VTs ( $291 \pm 49$  ms) were induced in 25 pigs. Mid-diastolic electrograms were recorded in the endocardium (endocardial VT) in 17 and in the epicardium (epicardial VT) in 13. Epicardial SI mapping showed that

scar area was similar in animals with and without epicardial VT ( $24 \pm 6$  cm<sup>2</sup> vs  $25 \pm 12$  cm<sup>2</sup>), but HT covered a higher surface of the epicardial scar in animals with VT ( $76 \pm 6\%$  vs  $61 \pm 10\%$ ,  $P = .03$ ). A patchy scar pattern was observed in all animals with epicardial VT but only in 3 animals without VT ( $P < .001$ ).

**CONCLUSION** CeMRI-based SI mapping allows identification of the epicardial VT substrate.

**KEYWORDS** Epicardium; Magnetic resonance imaging; Ventricular tachycardia; Arrhythmogenic substrate

**ABBREVIATIONS** 3D = 3-dimensional; CC = conduction channels; ceMRI = contrast-enhanced magnetic resonance imaging; CL = cycle length; EIC-LP = electrograms with isolated components/late potentials; ENDO = entire endocardium; ENDO-50% = internal half of the endocardium; EPI = entire epicardium; EPI-50% = external half of the epicardium; HT = heterogeneous tissue; LV = left ventricle; MRI = magnetic resonance imaging; PES = programmed electrical stimulation; SI = signal intensity; SMVT = sustained monomorphic ventricular tachycardia; VT = ventricular tachycardia

(Heart Rhythm 2014;11:1456–1464) © 2014 Heart Rhythm Society. All rights reserved.

This study was partially supported by the National Fund for Health Research (Fondo de Investigación Sanitaria) through Grants PI10/02771, TIN2007-68048-C02-01, TIN2007-68048-C02-02, and TEC2010-21619-C04-03 from the Spanish Ministry of Science and Innovation and the Cooperative Cardiovascular Disease Research Network (RECAVA), Instituto de Salud Carlos III, Ministry of Health. Dr. Arenal is a consultant for Medtronic and Boston Scientific, Spain **Address reprint requests and correspondence:** Dr. Ángel Arenal, Electrophysiology Unit, Cardiology Department, Hospital General Universitario Gregorio Marañón, 46 Dr. Esquerdo St, 28007 Madrid, Spain. E-mail address: arenal@secardiologia.es.

## Introduction

The substrate of most sustained monomorphic ventricular tachycardias (SMVTs) is located in the endocardium, but some ventricular tachycardias (VTs) can only be ablated from the epicardium.<sup>1–4</sup> A combined endo-epicardial substrate ablation approach reduces VT recurrences; however, <30% of patients in whom the epicardium was explored had an epicardial VT substrate.<sup>5</sup> In addition, epicardial fat may reduce voltage mapping accuracy to delimit epicardial scars.

Contrast-enhanced magnetic resonance imaging (ceMRI) reliably identifies scars and VT substrate: (1) infarct morphology, scar surface extension, and heterogeneous tissue (HT)

mass are predictors of VT inducibility and mortality<sup>6–8</sup>; and (2) VT-related endocardial slow conduction channels (CC)<sup>9,10</sup> correspond with HT channels that are detected by ceMRI-based signal intensity (SI) mapping, a method in which the averaged subendocardial tissue SI is projected onto a 3-dimensional (3D) left ventricular (LV) endocardial shell.<sup>11,12</sup>

We hypothesized that epicardial SMVT substrate can be identified by ceMRI-based endo–epicardial SI mapping. This hypothesis was assessed in a swine model of postinfarction VT. The purposes of the study were (1) to evaluate the capability of SI mapping to identify epicardial VT substrate, (2) to compare the characteristics of epicardial and endocardial VT substrates, and (3) to determine the time to epicardial VT substrate appearance.

## Methods

### Experimental protocol

The study protocol was approved by the Institutional Animal Care and Use Committee (Centro de Cirugía de Mínima Invasión Jesús Usón). Experimental details are available in the [Online Supplementary Material](#).

Thirty-one domestic pigs weighing 29 to 37 kg were used for this study. To induce closed chest myocardial infarction, the left anterior descending coronary artery was occluded transiently by a balloon catheter placed just distal to the first diagonal branch for 150 minutes, followed by reperfusion. CeMRI and electrophysiologic study were performed either 4 weeks (group 1) or 16 weeks (group 2) later in order to establish the time to epicardial VT substrate appearance.

### MRI acquisition and processing ([Online Supplementary Material](#))

The animals underwent ceMRI with a 1.5-T scanner (Intera, Philips Medical Systems, Best, The Netherlands). All images were obtained with ECG gating and breath-holding.

The MRI study consisted of cine steady-state free-precession imaging of LV function and late enhancement imaging of myocardial scar tissue. Late-enhanced images were obtained 15 minutes after a total injection of 0.2 mmol/kg of gadobutrol (Gadovist, Bayer Shering Pharma AG, Berlin, Germany) and were used for infarct characterization. Delayed enhancement data acquisition provided a pixel resolution of  $1.29 \times 1.29$  mm in-plane and a slice thickness of 2.5 mm, which corresponds to approximately 40 slices covering the LV. We used previously defined SI thresholds to quantify 2 different areas within the infarct zone: (1) the scar core defined by a SI  $>3$  SD above the mean of the remote normal myocardium, and (2) HT (i.e., gray zone) defined by an SI between 2 and 3 SD.<sup>7,8</sup>

### Magnetic resonance based endo–epicardial SI mapping

The myocardial wall was divided into 2 equal parts: subendocardium and subepicardium. The averaged SI of the internal half of the subendocardium (ENDO-50%), the entire subendocardium (ENDO), the entire subepicardium (EPI), and the external half of subepicardium (EPI-50%)

were projected respectively onto 3D endocardial and epicardial shell reconstructions of the LV to identify the endocardial and epicardial VT substrate. LV endocardial/epicardial contours were manually defined on contiguous short-axis slices using QMass MR 7.0 and imported into our tool in which 3D endocardial/epicardial reconstructions were computed offline from a short-axis ceMRI image volume using custom software developed in the MATLAB environment (Mathworks, Natick, MA). The 3D visualization interface was implemented in Java (Sun Microsystems, Santa Clara, CA) using VTK (Kitware, Clifton Park, NY) visualization algorithms.<sup>11</sup> These 4 surface maps were analyzed to determine the structure of the scar (endo–epicardial SI mapping; [Figure 1, A–D](#)). These surfaces were color coded to provide information on SI. The red area represented dense scar and was defined by  $SI \geq$  minimal SI in the core of the scar; the magenta area represented normal myocardium ( $SI \leq$  peak SI in normal myocardium); and the area between these extremes represented HT. In all SI maps, the extension of scar, dense scar, and HT were measured using custom-developed software. An HT channel was defined as a corridor of HT differentiated by a SI lower than the surrounding scar tissue ([Figure 1](#)). A patchy scar pattern was defined by the presence of at least 3 dense scar islets surrounded by HT; this implied the existence of at least 2 HT channels. For side-to-side comparison with voltage mapping, the scar extension and the orientation referred to the mitral annulus and segment location of each HT channel were determined.<sup>13</sup> Two independent investigators blind to the electrophysiologic study analyzed the SI maps.

### Electrophysiologic study and electroanatomic mapping

The animals underwent electrophysiologic study 2 days after ceMRI. A quadripolar catheter was placed at the right ventricular apex against the distal septum close to the infarct area. A multipolar catheter was placed in the pericardial sac as previously described.<sup>14</sup>

Point-by-point sequential endocardial and epicardial mapping was performed during sinus rhythm or right ventricular pacing using the CARTO system (XP version, Biosense Inc, Diamond Bar, CA) with the NaviStar ThermoCool catheter (Biosense Inc). Multiple sites were explored to obtain a minimal fill threshold of 10 mm in the low-voltage area; 0.5 and 1.5 mV were the limits to define dense scar and scar areas, respectively. As the upper and lower limits of the color range were set at 1.51 and 1.5 and then lowered in steps of 0.1 mV to 0.11 and 0.10 mV, 30 voltage maps were analyzed for each animal: 15 maps from the endocardium and 15 from the epicardium.

Slow CC and the activation sequence within CC were defined as referred<sup>9</sup> and tagged in the scar. In those cases in which voltage mapping was performed during sinus rhythm, CC were reviewed during right ventricular pacing to uncover electrograms with isolated components/late potentials (EIC-LP).<sup>15</sup> HT conduction velocity was estimated in CC in which



**Table 1** Comparison of endocardial and epicardial scar extension obtained by contrast-enhanced magnetic resonance imaging

	Endocardium	Epicardium	P value
Healthy tissue (cm <sup>2</sup> )	68 ± 11	99 ± 14	.001*
Total scar (cm <sup>2</sup> )	25 ± 9	24 ± 8	NS
Dense scar (cm <sup>2</sup> )	9 ± 5	7 ± 5	.008*
Heterogeneous tissue (cm <sup>2</sup> )	16 ± 5	17 ± 7	NS

\*p < .05.

multipolar catheter was placed in the pericardium over the scar. Programmed electrical stimulation (PES) was performed using a protocol that included 4 extrastimuli delivered after a drive cycle length (CL) at 600, 400, and 350 ms.<sup>16</sup>

When a VT was induced, endocardial and epicardial mapping were performed sequentially focusing on the scar. When mid-diastolic electrograms were recorded, entrainment mapping was attempted from these electrograms. After VT mapping of both scar surfaces, VT was terminated by pacing. Pacing from mid-diastolic electrogram sites was performed during sinus rhythm for further characterization of VT isthmuses (see [Online Supplementary Material](#)). PES was repeated from different locations, including the LV and epicardium, trying to induce a different tachycardia. If after 3 sets of PES only 1 VT was induced, we concluded that no other VT was inducible. Presystolic and mid-diastolic electrograms were tagged in voltage maps. Operators were blinded to the ceMRI images.

**Comparison of voltage and SI mapping**

SI and voltage maps were compared to establish the location of VT substrate and mid-diastolic electrograms in SI maps (see [Online Supplementary Material](#)). Agreement between SI and voltage maps was graded as high, intermediate, or low and considered separately for endocardial and epicardial surfaces. High concordance implied that all the HT had a corresponding CC and that scar in SI maps (SI >2 SD) and scar in voltage

**Table 2** Comparison between animals with and without epicardial VT

	Epicardial VT (n = 13)	No epicardial VT (n = 14)	P value
<b>Electroanatomic maps</b>			
Area <1.5 mV (cm <sup>2</sup> )	66 ± 37	58 ± 37	NS
Area <0.5 mV (cm <sup>2</sup> )	30 ± 20	24 ± 20	NS
Conduction channels <sup>†</sup>			.009*
0	0 (0%)	4 (21%)	
1	3 (23%)	7 (50%)	
Patchy pattern (≥ 2 channels)	10 (77%)	3 (29%)	
<b>MRI measurements</b>			
LV ejection fraction (%)	39 ± 6	34 ± 7	.04*
LV ED volume (ml)	147 ± 28	151 ± 28	NS
LV ES volume (ml)	89 ± 20	100 ± 22	NS
LV mass (g)	72 ± 17	72 ± 10	NS
LV mass > 2 SD (g)	13 ± 4	16 ± 7	NS
LV mass > 3 SD (g)	11 ± 4	12 ± 6	NS
<b>Signal intensity maps</b>			
Dense scar EPI-50% (cm <sup>2</sup> )	5 ± 2	10 ± 6	.01*
HT EPI-50% (cm <sup>2</sup> )	19 ± 5	14 ± 6	.07
Total scar EPI-50% (cm <sup>2</sup> )	24 ± 6	25 ± 12	NS
Healthy tissue EPI-50% (cm <sup>2</sup> )	99 ± 13	98 ± 16	NS
Dense scar/total scar EPI-50% (%)	23 ± 6	38 ± 2	.003*
HT/total scar EPI-50% (%)	76 ± 6	61 ± 10	.03*
HT structure EPI-50% <sup>†</sup>			.001*
No channel	0 (0%)	5 (36%)	
1 Channel	0 (0%)	4 (28%)	
Patchy pattern (≥ 2 channels)	13 (100%)	5 (36%)	

ED = end-diastolic; EPI = entire epicardium; EPI-50% = external half of the epicardium; ES = end-systolic; HT = heterogeneous tissue; LV = left ventricle; MRI = magnetic resonance imaging; VT = ventricular tachycardia.

\*P < .05.

<sup>†</sup>χ<sup>2</sup> test.

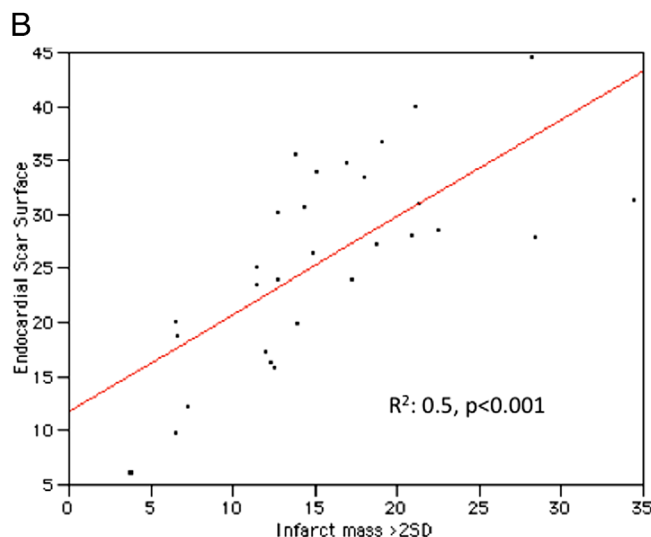
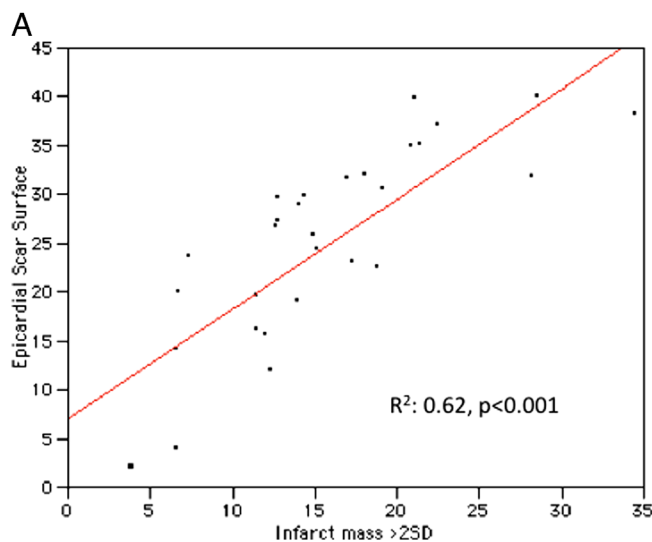


**Figure 2** Regression lines of the epicardial (A) and endocardial (B) scar extension in signal intensity (SI) maps and infarct mass. These regression lines show the correlation between the scar areas (>2 SD) in EPI-50% and ENDO-50% SI maps and infarct mass (>2 SD). Abbreviations as in [Figure 1](#).

maps (<1.5 mV) spanned the same segments.<sup>13</sup> Intermediate concordance meant that all HT channels and CC coincided but segment scar extension was different. In low concordance, only some HT channels and CC matched.

**Statistical analysis**

Values are given as mean ± SD. Comparisons were made using the *t* test, paired *t* test, and Fisher exact test. Linear

regression was used to estimate the relation between continuous variables. *P* < .05 was considered significant.

**Results**

Of the 31 animals included in the study, 2 died during coronary occlusion and 1 during electrophysiologic study before electroanatomic mapping was performed. Therefore, ceMRI was performed in 29 animals and electrophysiologic study in 28, in which LV ejection fraction was 36% ± 7%,

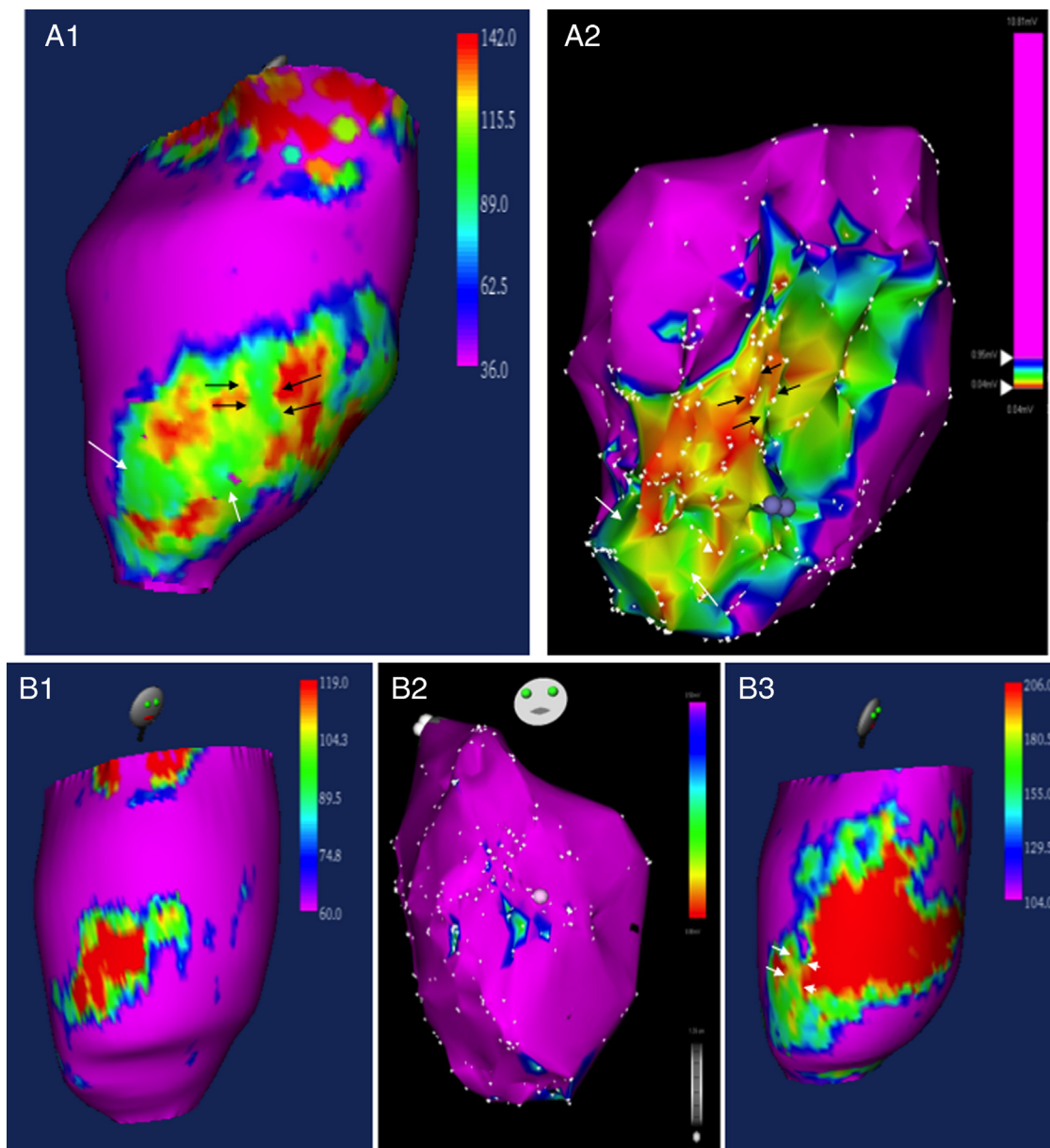


**Figure 3** Upper panel: EPI-50% and voltage maps of an experiment with inducible epicardial ventricular tachycardia (VT). The signal intensity (SI) map (A1) shows the scar and the patchy pattern with at least 3 dense scar islets surrounded by heterogeneous tissue (HT) channels. Although the location of HT channels is similar to the location of conduction channels (CC) in the voltage map (A2). Note that the CC marked by black arrows is incomplete because it does not cross the scar. Further anatomic evaluation of the explanted heart showed that this channel was partially covered by the fat surrounding the left anterior descending coronary artery so that voltage mapping could not detect the full length of the CC (see Figure 5). Dots indicate the site where mid-diastolic electrograms were recorded. Lower panel: EPI-50% and voltage maps of experiments without inducible epicardial VT. One experiment shows a small scar core with minimal extension of HT in both the SI (B1) and voltage maps (B2). The other experiment shows a large scar core with a single isolated small channel (arrows) and minimal extension of HT in the SI map (B3). Other abbreviations as in Figure 1.

LV mass  $72 \pm 13$  g, LV mass with SI  $>2$  SD was  $15 \pm 6$  g, and LV mass with SI  $>3$  SD was  $12 \pm 5$  g. Fifteen animals belonged to group 1 and 13 to group 2.

### Electrophysiologic study

Thirty-three different SMVTs ( $291 \pm 49$  ms) were induced in 25 pigs, and presystolic or mid-diastolic electrograms were recorded in 30 VT. Seventeen VTs were considered endocardial VTs because mid-diastolic electrograms were recorded in the endocardium; in 2 of these VTs mid-diastolic electrograms were also recorded at the epicardium but for the analysis were considered endocardial VT. Thirteen VTs were classified as epicardial because mid-diastolic electrograms were only recorded at the epicardium. The epicardial VT CL was significantly longer than endocardial VT CL ( $329 \pm 49$  vs  $267 \pm 31$  ms,  $P = .003$ ).

### Electroanatomic mapping

Endocardial voltage mapping was obtained in 28 experiments and epicardial voltage mapping in 27 (in 1 animal pericardial adhesences precluded mapping). Epicardial and endocardial maps were created with  $477 \pm 156$  points and  $549 \pm 198$  points, respectively. Both the scar and dense scar were larger at the epicardium ( $59 \pm 35$  cm<sup>2</sup> vs  $41 \pm 15$  cm<sup>2</sup>,  $P = .01$ ; and  $25 \pm 19$  cm<sup>2</sup> vs  $11 \pm 8$  cm<sup>2</sup>,  $P < .001$ ). Thirty-six epicardial CC in 22 animals and 47 endocardial CC in 26 animals were found. EIC-LP were recorded in all channels during sinus rhythm or ventricular pacing (Figure 1F). The activation time of the latest component of the electrograms located in the inner part of the channels was longer in epicardial than in endocardial CC ( $146 \pm 37$  ms vs  $115 \pm 34$  ms,  $P < .001$ ). The estimated HT conduction velocity in CC was slower in the epicardium ( $0.28 \pm 0.05$  m/s vs  $0.54 \pm 0.21$  m/s,  $P = .02$ ).

### SI mapping

Table 1 lists the endocardial and epicardial extension of the scar, scar core and HT. Endocardial and epicardial scar surface areas in SI mapping correlate significantly with scar tissue mass (Figure 2). In 21 animals, 44 and 26 epicardial HT channels were identified in EPI-50% SI and EPI SI maps, respectively. Similarly, a patchy pattern was more frequently observed in EPI-50% (17 vs 10 maps). Thirty-five endocardial HT channels in 25 animals were detected in ENDO-50% SI maps but only 27 HT channels in 20 animals in ENDO SI maps. Because the ventricular wall at the infarcted zone ranged from 8 to 12 mm, these data suggest that averaging 2 to 3 mm of the external epicardium or internal endocardium is more sensitive than averaging the entire epicardium or endocardium.

### Characteristics of epicardial VT substrate

An epicardial VT was induced in 13 animals: 6 in group 1 and 7 in group 2 ( $P = \text{NS}$ ). In all VTs, mid-diastolic electrograms were recorded at or near ( $<10$  mm) the CC. VT isthmus identification was based on (1) concealed entrainment and a postpacing interval equal to the VT CL in 2 VTs, (2) pacing

from mid-diastolic sites during sinus rhythm reproducing VT QRS morphology and a similar stimulus-QRS interval to electrogram-QRS interval during tachycardia in 8 VTs, and (3) mid-diastolic electrograms in 3 VT (see Online Supplementary Material). Table 2 lists the differences between animals with and those without epicardial VT: (1) the dense scar area was smaller, (2) the proportion of HT was higher, and (3) a “patchy” scar pattern was identified in all experiments with induced VT but in only 36% of the animals without inducible VT (Figures 1 and 3). It also seems that a minimal dense scar extension is needed to lodge a VT as only 1 of 6 animals with a total scar  $<19$  cm<sup>2</sup> had inducible VT (Figure 3, bottom panel, and Online Supplementary Figure 1).

### Characteristics of endocardial VT substrate

Table 3 lists the differences between animals with and those without endocardial VT. An endocardial VT was induced in 17 animals: 8 in group 1 and 9 in group 2

**Table 3** Comparison between animals with and without endocardial VT

	Endocardial VT (n = 17)	No endocardial VT (n = 11)	P value
<b>Electroanatomic maps</b>			
Area $<1.5$ mV (cm <sup>2</sup> )	$48 \pm 12$	$36 \pm 20$	.1
Area $<0.5$ mV (cm <sup>2</sup> )	$13 \pm 8$	$11 \pm 10$	NS
Conducting channels <sup>†</sup>			.02*
0	0 (0%)	2 (18%)	
1	14 (82%)	4 (36%)	
Patchy pattern ( $\geq 2$ channels)	3 (18%)	5 (45%)	
<b>MRI measurements</b>			
LV ejection fraction (%)	$34 \pm 7$	$39 \pm 5$	.06
LV ED volume (ml)	$183 \pm 28$	$143 \pm 31$	NS
LV ES volume (ml)	$100 \pm 20$	$86 \pm 22$	.1
LV mass (g)	$72 \pm 10$	$72 \pm 71$	NS
LV mass $>2$ SD (g)	$16 \pm 5$	$12 \pm 5$	0.09
LV mass $>3$ SD (g)	$12 \pm 5$	$10 \pm 6$	NS
<b>Signal intensity maps</b>			
Dense scar ENDO-50% (cm <sup>2</sup> )	$11 \pm 4$	$8 \pm 5$	.1
HT ENDO-50% (cm <sup>2</sup> )	$16 \pm 5$	$14 \pm 5$	NS
Total scar ENDO-50% (cm <sup>2</sup> )	$27 \pm 8$	$22 \pm 9$	.1
Healthy tissue ENDO-50% (cm <sup>2</sup> )	$67 \pm 10$	$68 \pm 18$	NS
Dense scar/total scar ENDO-50% (%)	$37 \pm 10$	$32 \pm 10$	.1
HT/total scar ENDO-50% (%)	$62 \pm 10$	$67 \pm 10$	.1
HT structure ENDO-50% <sup>†</sup>			.02*
No channel	0 (0%)	3 (28%)	
1 Channel	14 (82%)	4 (36%)	
Patchy pattern ( $\geq 2$ channels)	3 (18%)	4 (36%)	

ED = end-diastolic; ENDO = entire endocardium; ENDO-50% = internal half of the endocardium; ES = end-systolic; HT = heterogeneous tissue; LV = left ventricle; MRI = magnetic resonance imaging; VT = ventricular tachycardia.

\* $P < .05$ .

<sup>†</sup>Chi-square test.

( $P = NS$ ). In all but 1 VT, presystolic or mid-diastolic electrograms were recorded at the inner part or exit of CC. VT isthmus identification was based on (1) concealed entrainment and a postpacing interval equal to the VT CL in 4 VTs, (2) pacing from mid-diastolic sites during sinus rhythm reproducing VT QRS morphology and a similar stimulus-QRS interval to electrogram-QRS interval during tachycardia in 8 VTs, and (3) mid-diastolic electrograms in 5 VT (see [Online Supplementary Material](#)). All animals with inducible endocardial VT had at least 1 HT channel in ENDO-50% SI maps. In 3 of these animals with inducible endocardial VTs, no HT channels were observed in ENDO SI maps.

Endocardial VTs were more frequently induced in experiments with a single CC or HT channel than with a patchy pattern ([Figure 4](#)).

### Comparison of SI and voltage mapping

When EPI-50% and ENDO-50% SI maps were compared with their corresponding voltage maps, high, intermediate, or low concordance was found in 8, 17, and 3 endocardial maps and in 8, 12, and 7 epicardial maps. The low concordance in >25% of epicardial maps ([Figure 3, A1 and A2](#)) was mainly due to the effect of epicardial fat on voltage mapping ([Figure 5](#)).

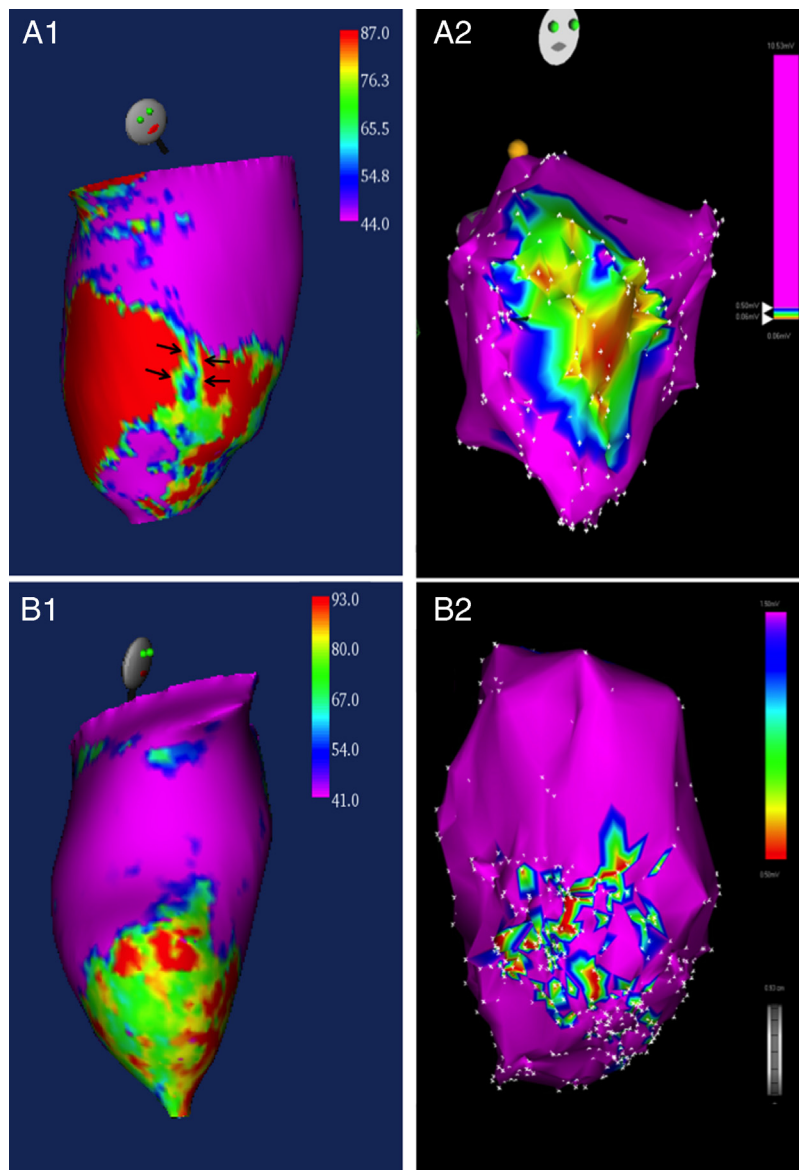


**Figure 4** **Upper panel:** ENDO-50% of an experiment with inducible endocardial ventricular tachycardia (VT). **A1:** Signal intensity (SI) maps show the scar and the heterogeneous tissue (HT) channel in 1 experiment with endocardial VT induction. The HT channel runs perpendicular to the mitral valve between 2 large scar cores suggesting the presence of a large circuit (*arrows*). This channel is also observed in the voltage maps (**A2**). **Lower panel:** ENDO-50% of an experiment without inducible endocardial VT. **B1:** The SI map shows minimal islets of dense scar from an experiment with no VT. There are several possible circuits, but the length of these circuits is shorter than those found in [Figure 5](#). **B2:** The voltage map shows the scar with voltage scar cutoffs set at 0.5/1.5 mV. Note the small patches of scar. Abbreviations as in [Figure 1](#).

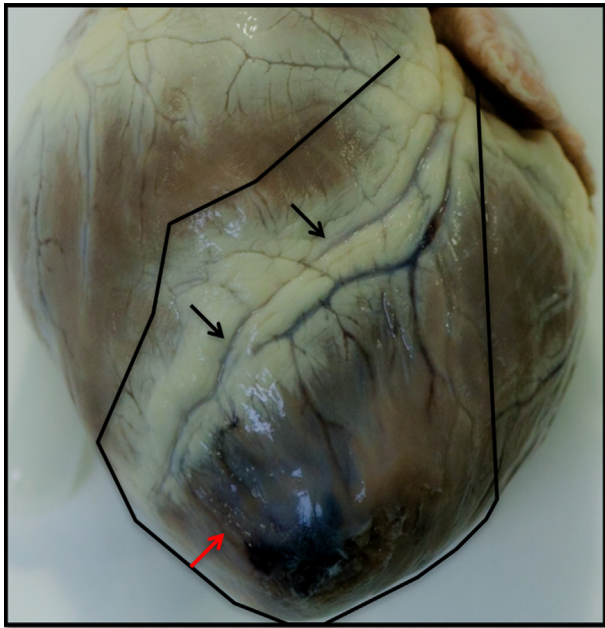


**Figure 5** Explanted heart corresponding to animal in Figure 3, upper panel. The black line encircles the infarcted area. The black arrows show the area where epicardial fat seems to prevent channel identification with voltage mapping (black arrows in Figure 3, A2). The red arrow shows the heterogeneous tissue surrounding the apex (white arrows in Figure 3, A2), which is better differentiated due to the absence of fat.

## Discussion

This study shows that (1) epicardial VT substrate can be identified by ceMRI-based SI mapping, (2) a patchy scar pattern is associated with epicardial VT inducibility, (3) epicardial and endocardial VT substrates are different, (4) SI and voltage mapping concordance is affected by epicardial fat, and (5) epicardial VT substrate appears shortly after myocardial infarction.

## Experimental model

This experimental model is characterized by high epicardial VT inducibility. Prolonged coronary occlusion likely is the cause for the wide epicardial scar extension and VT inducibility. All induced VTs were monomorphic as opposed to data from previous studies in which many fast, focal VTs were induced.<sup>17</sup> The PES protocol used in this study, which is very sensitive and specific, could explain these differences.<sup>16</sup> Amiodarone, which was stopped 3 days after infarct induction, could not have had any effect on the induced VT. In this model, VTs usually are related to CC, and, although a recent study has raised some concerns about the relation of channels and VT isthmuses,<sup>18</sup> in the referred study VTs with isthmuses not located within channels were very slow (VT CL  $440 \pm 40$  ms), whereas fast VTs usually were related to channels (VT CL  $377 \pm 67$  ms). In our study, VT CL was  $291 \pm 49$  ms.

## Epicardial VT substrate and SI mapping

Several studies have demonstrated ceMRI is a reliable method for identifying endocardial VT substrate: infarct

surface extension was a better predictor of inducible VT than LV ejection fraction,<sup>6</sup> VT critical sites are always confined to areas of high SI,<sup>18,19</sup> and there is correlation of VT-related CC and HT channels detected by SI mapping.<sup>11</sup>

Epicardial VT appears in scars characterized by a complex patchy geometry with a higher proportion of HT. The probability of inducing an epicardial VT when a “patchy” scar pattern is present is  $>70\%$ . Averaging a layer of 2 to 3 mm of the external half of the subepicardium SI is likely a better cutoff for identifying the epicardial VT substrate than averaging the entire subepicardium.

## Epicardial and endocardial VT substrate differences

The longer activation time of late potential at the epicardium could be explained by (1) transmural delay during sinus rhythm as the activation goes from endocardium to epicardium and (2) the slower epicardial HT conduction velocity secondary to the lack of Purkinje fibers and the differences in action potentials.<sup>20</sup> This slow conduction velocity could favor induction of slower VT even in the absence of large obstacles as it happens in patchy scars. On the other hand, endocardial VT substrate is characterized by large dense scars. Endocardial fast conduction probably requires larger obstacles to maintain stable reentries.

## Study limitations

The complete reentrant circuit was not mapped because the induced VT were very fast (mean CL 291 ms) and usually poorly tolerated. Nevertheless, as mapping was focused on the scar area, presystolic or mid-diastolic electrograms were identified in the majority of the experiments.

Although radiofrequency ablation was not performed because of the previously reported high risk of developing ventricular fibrillation<sup>21</sup> and information concerning VT termination sites is not available, mapping and pacing maneuvers including concealed entrainment reinforced the precise location of the VT isthmus.

The endocardium of the distal septum of the right ventricle was not systematically mapped. As this area could be affected by coronary occlusion and could correspond with some areas of the epicardial SI mapping, we must assume certain limitations when comparing epicardial voltage and SI maps in this particular segment.

Most patients requiring VT ablation have an implantable cardioverter-defibrillator, which is still considered a contraindication for MRI. Nevertheless, recent studies have shown that ceMRI can be performed safely in selected patients.<sup>22</sup>

## Clinical implications

Our results suggest that ceMRI-based endo–epicardial SI mapping could facilitate the ablation procedure by (1) identifying the patients in whom the VT substrate extends to the epicardium and (2) helping to interpret epicardial voltage maps when epicardial fat is supposed to have altered the scar

delimitation. These observations support clinical studies to define the role of ceMRI in postinfarction VT ablation.

## Acknowledgments

We thank Antonio Moratalla and Alicia Barrio for technical assistance, and Thomas O'Boyle for language revision.

## Appendix

### Supplementary data

Supplementary data associated with this article can be found in the online version at <http://dx.doi.org/10.1016/j.hrthm.2014.04.022>.

## References

- Brugada J, Berruezo A, Cuesta A, Osca J, Chueca E, Fosch X, Wayar L, Mont L. Nonsurgical transthoracic epicardial radiofrequency ablation: an alternative in incessant ventricular tachycardia. *J Am Coll Cardiol* 2003;41:2036–2043.
- Della Bella P, Brugada J, Zeppenfeld K, Merino J, Neuzil P, Maury P, Maccabelli G, Vergara P, Baratto F, Berruezo A, Wijngaarden AP. Epicardial ablation for ventricular tachycardia: a European multicenter study. *Circ Arrhythm Electrophysiol* 2011;4:653–659.
- Sacher F, Roberts-Thomson K, Maury P, et al. Epicardial ventricular tachycardia ablation a multicenter safety study. *J Am Coll Cardiol* 2010;55:2366–2372.
- Sosa E, Scanavacca M, d'Avila A, Oliveira F, Ramires JAF. Nonsurgical transthoracic epicardial catheter ablation to treat recurrent ventricular tachycardia occurring late after myocardial infarction. *J Am Coll Cardiol* 2000;35:1442–1449.
- Di Biase L, Santangeli P, Burkhardt DJ, et al. Endo-epicardial homogenization of the scar versus limited substrate ablation for the treatment of electrical storms in patients with ischemic cardiomyopathy. *J Am Coll Cardiol* 2012;60:132–141.
- Bello D, Fieno DS, Kim RJ, Pereles FS, Passman R, Song G, Kadish AH, Goldberger JJ. Infarct morphology identifies patients with substrate for sustained ventricular tachycardia. *J Am Coll Cardiol* 2005;45:1104–1108.
- Yan AT, Shayne AJ, Brown KA, Gupta SN, Chan CW, Luu TM, Di Carli MF, Reynolds HG, Stevenson WG, Kwong RY. Characterization of the peri-infarct zone by contrast-enhanced cardiac magnetic resonance imaging is a powerful predictor of post-myocardial infarction mortality. *Circulation* 2006;114:32–39.
- Schmidt A, Azevedo CF, Cheng A, Gupta SN, Bluemke DA, Foo TK, Gerstenblith G, Weiss RG, Marban E, Tomaselli GF, Lima JA, Wu KC. Infarct tissue heterogeneity by magnetic resonance imaging identifies enhanced cardiac arrhythmia susceptibility in patients with left ventricular dysfunction. *Circulation* 2007;115:2006–2014.
- Arenal A, del Castillo S, Gonzalez-Torrecilla E, Atienza F, Ortiz M, Jimenez J, Puchol A, Garcia J, Almendral J. Tachycardia-related channel in the scar tissue in patients with sustained monomorphic ventricular tachycardias: influence of the voltage scar definition. *Circulation* 2004;110:2568–2574.
- Hsia HH, Lin D, Sauer WH, Callans DJ, Marchlinski FE. Anatomic characterization of endocardial substrate for hemodynamically stable reentrant ventricular tachycardia: identification of endocardial conducting channels. *Heart Rhythm* 2006;3:503–512.
- Perez-David E, Arenal A, Rubio-Guivernau JL, et al. Noninvasive identification of ventricular tachycardia-related conducting channels using contrast-enhanced magnetic resonance imaging in patients with chronic myocardial infarction: comparison of signal intensity scar mapping and endocardial voltage mapping. *J Am Coll Cardiol* 2011;57:184–194.
- Andreu D, Berruezo A, Ortiz-Perez JT, Silva E, Mont L, Borrás R, de Caralt TM, Perea RJ, Fernandez-Armenta J, Zeljko H, Brugada J. Integration of 3D electroanatomic maps and magnetic resonance scar characterization into the navigation system to guide ventricular tachycardia ablation. *Circ Arrhythm Electrophysiol* 2011;4:674–683.
- Josephson ME. *Clinical Cardiac Electrophysiology*. Third edition. Philadelphia: Lippincott Williams & Williams; 2002:457.
- Sosa E, Scanavacca M, D'Avila A, Piccioni J, Sanchez O, Velarde JL, Silva M, Reolao B. Endocardial and epicardial ablation guided by nonsurgical transthoracic epicardial mapping to treat recurrent ventricular tachycardia. *J Cardiovasc Electrophysiol* 1998;9:229–239.
- Arenal A, Glez-Torrecilla E, Ortiz M, Villacastin J, Fdez-Portales J, Sousa E, del Castillo S, Perez de Isla L, Jimenez J, Almendral J. Ablation of electrograms with an isolated, delayed component as treatment of unmappable monomorphic ventricular tachycardias in patients with structural heart disease. *J Am Coll Cardiol* 2003;41:81–92.
- Hummel JD, Strickberger SA, Daoud E, Niebauer M, Bakr O, Man KC, Williamson BD, Morady F. Results and efficiency of programmed ventricular stimulation with four extrastimuli compared with one, two, and three extrastimuli. *Circulation* 1994;90:2827–2832.
- Ashikaga H, Sasano T, Dong J, et al. Magnetic resonance-based anatomical analysis of scar-related ventricular tachycardia: implications for catheter ablation. *Circ Res* 2007;101:939–947.
- Codreanu A, Odille F, Aliot E, Marie PY, Magnin-Poull I, Andronache M, Mandry D, Djabballah W, Regent D, Felblinger J, de Chillou C. Electroanatomic characterization of post-infarct scars comparison with 3-dimensional myocardial scar reconstruction based on magnetic resonance imaging. *J Am Coll Cardiol* 2008;52:839–842.
- Desjardins B, Crawford T, Good E, Oral H, Chugh A, Pelosi F, Morady F, Bogun F. Infarct architecture and characteristics on delayed enhanced magnetic resonance imaging and electroanatomic mapping in patients with postinfarction ventricular arrhythmia. *Heart Rhythm* 2009;6:644–651.
- Akar FG, Spragg DD, Tunin RS, Kass DA, Tomaselli GF. Mechanisms underlying conduction slowing and arrhythmogenesis in nonischemic dilated cardiomyopathy. *Circ Res* 2004;95:717–725.
- Hogh Petersen H, Chen X, Pietersen A, Svendsen JH, Haunso S. Lesion dimensions during temperature-controlled radiofrequency catheter ablation of left ventricular porcine myocardium: impact of ablation site, electrode size, and convective cooling. *Circulation* 1999;99:319–325.
- Dickfeld T, Tian J, Ahmad G, Jimenez A, Turgeman A, Kuk R, Peters M, Saliaris A, Saba M, Shorofsky S, Juey J. MRI-Guided ventricular tachycardia ablation: integration of late gadolinium-enhanced 3D scar in patients with implantable cardioverter-defibrillators. *Circ Arrhythm Electrophysiol* 2011;4:172–184.